

Stereodynamical control of a quantum scattering resonance in cold molecular collisions

Pablo G. Jambrina

*Departamento de Química Física. Universidad de Salamanca, Salamanca 37008, Spain.**

James F. E. Croft

*The Dood-Walls Centre for Photonic and Quantum Technologies, Dunedin, New Zealand and
Department of Physics, University of Otago, Dunedin, New Zealand†*

Hua Guo

*Department of Chemistry and Chemical Biology,
University of New Mexico, Albuquerque, New Mexico 87131, United States‡*

Mark Brouard

*The Department of Chemistry, University of Oxford,
The Chemistry Research Laboratory, Oxford OX1 3TA, UK.§*

Naduvath Balakrishnan

Department of Chemistry and Biochemistry, University of Nevada, Las Vegas, Nevada 89154, USA¶

F. Javier Aoiz

*Departamento de Química Física. Universidad Complutense. Madrid 28040, Spain***

(Dated: April 30, 2022)

Cold collisions of light molecules are often dominated by a single partial wave resonance. For the rotational quenching of HD($v = 1, j = 2$) by collisions with ground state para-H₂, the process is dominated by a single $L = 2$ partial wave resonance centered around 0.1 K. Here, we show that this resonance can be switched on or off simply by appropriate alignment of the HD rotational angular momentum relative to the initial velocity vector, thereby enabling complete control of the collision outcome.

At cold (< 1 K) and ultracold (< 1 μ K) temperatures molecules can be prepared in precisely defined quantum states and interrogated with unprecedented precision. Recent developments in molecule cooling and trapping technologies [1–8] as well as merged or co-expanding beam techniques [9–14] have made it increasingly possible to study molecular systems at these low temperatures. Such systems have even been used in the frontiers of particle physics, [15] for example in the search for the electric dipole moment of the electron. [16–18] Cold and ultracold molecules therefore offer an ideal platform on which to precisely study fundamental aspects of molecular dynamics [19–22] such as the role of quantum statistics, [23] threshold laws [24] and geometric-phase effects. [25]

One of the most fundamental questions in molecular dynamics is the dependence of a collision outcome on the relative orientation and/or alignment of the reactants – the stereodynamics of a collision process. [26–34] At cold and ultracold temperatures, where collisions proceed through just one or a few partial waves, their stereodynamics can be studied at their most fundamental level – the single quantum state level. In a recent series of papers Perreault *et al.* have examined the role that the initial alignment of HD plays in cold collisions with H₂ and D₂ [35, 36]. Control over rotational quenching rates was demonstrated, and subsequent theoretical studies revealed that for certain states the scattering dy-

namics of cold HD+n-H₂ collisions is determined by a single ($L = 2$) partial-wave shape resonance at around 1 K [37, 38].

While the stereodynamics of atom-diatom collisions has been explored in previous theoretical studies [39–44], collisions between oriented and/or aligned molecules in cold conditions remain largely unexplored. In this work we apply the theoretical methods required to describe the stereodynamics of inelastic molecule-molecule collisions, specifically, to one of the prototypical systems recently studied by Perreault *et al.* – rotational quenching of HD in cold collisions with H₂. In particular, we will demonstrate how the stereodynamics of cold molecule-molecule collisions can be determined by a single partial wave shape resonance and how it can be used to obtain exquisite control of the collision outcome.

Quantum Mechanical (QM) inelastic scattering calculations were carried out using the time-independent coupled-channel formalism within the total angular momentum (TAM) representation of Arthurs and Dalgarno [45], which has previously been successfully applied to collisions of H₂ with H₂ [46–48] and HD [49–51]. The scattering calculations were performed using a modified version of the TwoBC code [52, 53] on the full-dimensional potential surface of Hinde [54]. In the TAM representation the rotational angular momenta of the dimers, \mathbf{j}_{H_2} and \mathbf{j}_{HD} , are coupled to form $\mathbf{j}_{12} =$

$\mathbf{j}_{\text{H}_2} + \mathbf{j}_{\text{HD}}$ which is in turn coupled with the orbital angular momentum \mathbf{L} to form the total angular momentum $\mathbf{J} = \mathbf{L} + \mathbf{j}_{12}$. Scattering calculations are performed separately for each value of the total angular momentum J and parity $I = (-1)^{j_{\text{H}_2} + j_{\text{HD}} + L}$ that reflects the inversion symmetry of the wavefunction [55], yielding the Scattering matrix, $S_{\gamma, \gamma'}^J$, labeled by the asymptotic entrance and exit channels γ and γ' respectively. The composite index $\gamma = v_{\text{HD}} j_{\text{HD}} v_{\text{H}_2} j_{\text{H}_2} L j_{12}$ denotes the vibrational and rotational quantum numbers of each dimer (v and j respectively), the orbital angular momentum (L), and the sum of the angular momenta of the dimers (j_{12}). The integral cross section for state-to-state rovibrationally inelastic collisions is then given in terms of the S-matrix by

$$\sigma_{\alpha \rightarrow \alpha'} = \frac{\pi}{(2j_{\text{H}_2} + 1)(2j_{\text{HD}} + 1)k_\alpha^2} \sum_{\gamma, \gamma'} (2J + 1) |\delta_{\gamma, \gamma'} - S_{\gamma, \gamma'}^J|^2, \quad (1)$$

where α is the combined molecular state, $\alpha = v_{\text{H}_2} j_{\text{H}_2} v_{\text{HD}} j_{\text{HD}}$, $k^2 = 2\mu E_{\text{col}}/\hbar^2$ is the square of the wave vector, E_{col} the collision energy, and μ the reduced mass. From the elements of the S-matrix, the scattering amplitudes, $f_{\alpha' \Omega', \alpha \Omega}$ where Ω (Ω') are the helicities, the projection of j (j') into the approach (recoil) direction, were determined using the procedure described in Ref 37.

Inelastic collisions of HD($v = 1, j = 2$) with H₂($v = 0, j = 0$) at low collision energies are dominated by $\Delta j = -1$ and -2 transitions in HD leading to HD($v' = 1, j' = 1$)+H₂ and HD($v' = 1, j' = 0$)+H₂, respectively. Vibrational de-excitation of HD is energetically allowed, but the cross section for vibrational relaxation is around 5-6 orders of magnitude smaller at these collision energies. Energetically, two-quanta rotational excitation of H₂ is not allowed.

The energy dependence of the rotational quenching cross sections is shown in the top panel of Fig. 1. It is seen that at the lowest energies considered, the cross section for $\Delta j = -1$ is about a factor of seven larger than for $\Delta j = -2$. Both show the onset of the Wigner threshold regime below about 0.01 K ($\propto E_{\text{col}}^{-1/2}$ for pure s -wave collisions). The most salient feature for $\Delta j = -1$ is the presence of a sharp resonance at 0.1 K, where the cross section increases by almost a factor of four. This is an $L = 2$ shape resonance (Fig. 1 shows the contribution from $L = 2$ separately), that is caused by a single S-matrix element corresponding to $L = 2$ and $J = 3$ in the TAM representation. As a consequence of this, the resonance has a defined parity, in this case the block that does not include $\Omega=0$, which as we will show later has important consequences for the collision mechanism. This particular resonance is not observed for $\Delta j = -2$, even though most of the scattering also comes from $L = 2$. Such resonances are ubiquitous features of inelastic and reactive collisions, especially in the cold regime. Here we

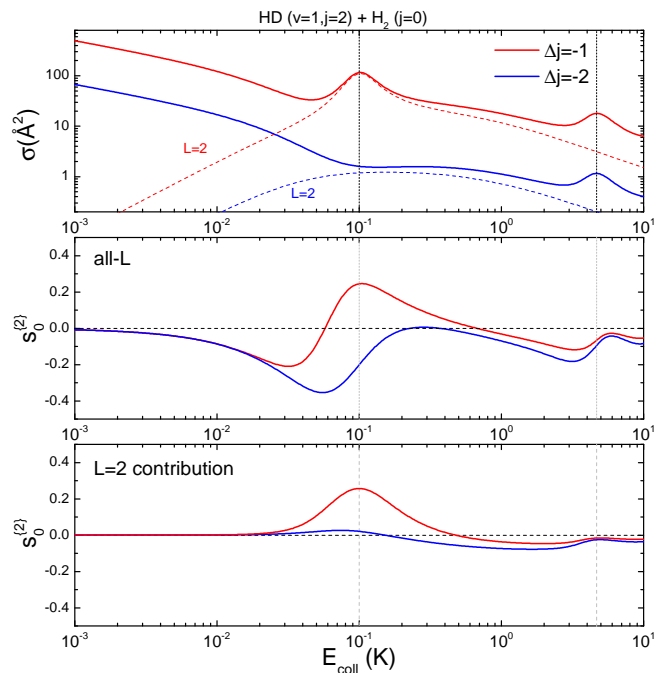


FIG. 1. Cross sections for the HD($v=1, j=2$) + H₂($v=0, j=0$) inelastic collisions as a function of the collision energy. Top panel: cross sections for $\Delta j = -1$ (solid red line) and $\Delta j = -2$ (solid blue line). The contributions of the $l=2$ partial wave to the cross sections are shown as dashed lines. Middle and bottom panels: Energy dependence of the $s_0^{(2)}$ integral alignment moment for $\Delta j = -1$ (red) and -2 (blue). In the middle panel the overall results are shown, while the contribution for $L = 2$ is displayed in the bottom panel.

show how they can be used to reveal the collision mechanism and, perhaps more importantly, *control the collision outcome*.

The concept of a collision mechanism can be at times somewhat vague, relying on qualitative rather than on quantitative results, which can lead to misinterpretations. To avoid any ambiguities we use the three-vector correlation $\mathbf{k} - \mathbf{j}_{\text{HD}} - \mathbf{k}'$ (where \mathbf{k} and \mathbf{k}' are the initial and final relative wave vectors) which is especially well-suited to characterizing collision mechanisms within a purely quantum-mechanical framework. More explicitly we use the set of reactant polarization parameters, $s_q^{\{k\}}$, of rank k and component $q = -k \dots k$, which define the vector correlation [56]. For the present purposes, the most relevant of these parameters is $s_0^{\{2\}}$, the first alignment moment of \mathbf{j} about the incoming relative velocity. Its value specifies the direction of the rotational angular momentum relative to the initial approach. Negative values of $s_0^{\{2\}}$ indicate a preference for head-on collisions (rotational angular momentum \mathbf{j}_{HD} perpendicular to \mathbf{k}), whereas positive values indicate a preference for side-on collisions (\mathbf{j}_{HD} mostly parallel to \mathbf{k}). The polarization parameters are calculated from the integra-

tion of the polarization-dependent differential cross sections, $S_q^{\{k\}}(\theta)$, over the scattering angle, θ . For the $\mathbf{k} - \mathbf{j}_{\text{HD}} - \mathbf{k}'$ correlation the $S_q^{\{k\}}(\theta)$ can be determined from $f_{\alpha'\Omega',\alpha\Omega}$: [57]

$$S_q^{\{k\}}(\theta) = \frac{1}{2j_{\text{HD}} + 1} \sum_{\Omega_1 \Omega_2} \sum_{\Omega'} f_{\alpha'\Omega',\alpha\Omega_1} [f_{\alpha'\Omega',\alpha\Omega_2}]^* \times \langle j_{\text{HD}} \Omega_1, kq | j_{\text{HD}} \Omega_2 \rangle \quad (2)$$

where $\langle \dots | \dots \rangle$ denotes the Clebsch-Gordan coefficient. In the particular case of $q=0$, the $s_q^{\{k\}}$ can also be obtained directly from the S-matrix elements [58].

The middle panel of Fig. 1 shows the polarization moment $s_0^{\{2\}}$ as a function of the collision energy for both the $\Delta j = -1$ and -2 transitions. At the lowest energies, the moment goes to zero, as required for ultracold collisions [59]. With increasing collision energy, $s_0^{\{2\}}$ takes negative values for both transitions, showing a preference for head-on encounters. However, at the proximity of the resonance, $s_0^{\{2\}}$ exhibits markedly different behavior for the two transitions. It turns positive for $\Delta j = -1$ peaking at the energy of the resonance (denoted with a vertical dashed line), while for $\Delta j = -2$ it remains negative. This shows that the resonance for $\Delta j = -1$ is associated with a specific mechanism that is not shared by the $\Delta j = -2$ transition. At energies above the resonance, $s_0^{\{2\}}$ again shows the same trend for both transitions, with a small change around 4.75 K caused by a second resonance (present in both Δj transitions) that does not change the mechanism significantly.

To unambiguously analyze the effect of the resonance, the $L = 2$ contribution to $s_0^{\{2\}}$ is shown in the bottom panel of Fig. 1. It is calculated by including only the $L = 2$ elements of the scattering matrix (without considering their coherence with other L values). Regardless of Δj , the $L = 2$ contribution to $s_0^{\{2\}}$ goes to zero at ultracold energies, as does $\sigma_{L=2}$ (see top panel). Moreover, up to 0.5 K, including the resonance, the sign of the $L = 2$ contribution to $s_0^{\{2\}}$ is positive (favoring side-on collisions) while it is negative for higher collision energies. Although at the resonance the sign of the $L=2$ contribution to $s_0^{\{2\}}$ is positive for both $\Delta j=-1$ and -2 , its magnitude is much larger for the former. Since, $L = 2$ collisions dominate around 0.1 K for both Δj (see top panel of Fig. 1), these results indicate that the overall change of $s_0^{\{2\}}$, and hence of the collision mechanism, is caused by the resonance and not due to a larger contribution of $L = 2$.

The distinct mechanism for the resonance suggests that it might be possible to suppress its effect by appropriate state-preparation of the HD rotational angular momentum [35, 36]. The cross sections for different extrinsic preparations can be computed following the procedure described in Ref. 57. If HD is prepared in a directed state, $m=0$, where m is the magnetic quantum number,

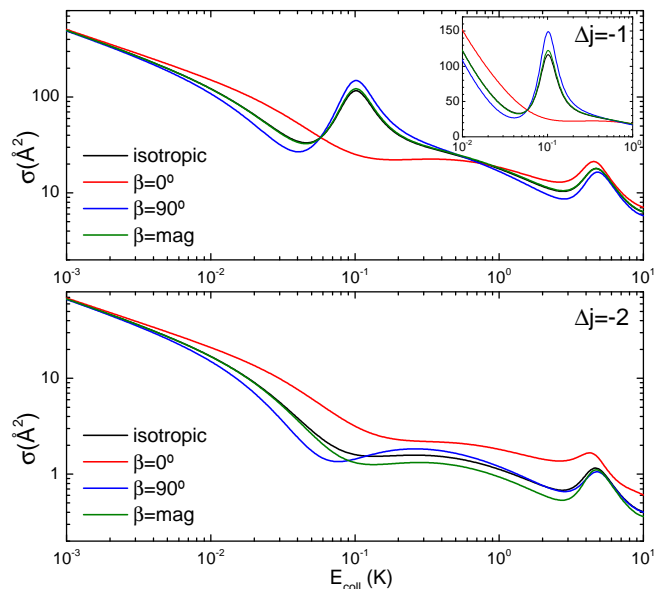


FIG. 2. Top panel, cross sections as a function of the collision energy for $\Delta j = -1$ for different preparations of the HD internuclear axis, $\beta = 0^\circ$ (red line), $\beta = 90^\circ$ (blue line), and the magic angle (olive line). The isotropic preparation (in absence of external alignment) is shown in black. The inset shows a zoom of the resonance region in a linear ordinate-axis scale. Bottom panel: Same as top panel but for $\Delta j = -2$.

it leads to the alignment of the internuclear axis along the quantization axis (in the case of refs. 35, 36 the polarization vector of the pump and Stokes lasers). By varying the direction of the laboratory-fixed axis with regard to the scattering frame it is possible to change the external preparations generating different relative geometries of the reactants prior the collision. We will label the different extrinsic preparations using β and α , where β is the polar angle between the polarization vector and the initial relative velocity, and α is the azimuthal angle that defines the direction of the polarization vector with respect to the $\mathbf{k} - \mathbf{k}'$ frame. Accordingly, $\beta = 0^\circ$ implies head-on collisions while $\beta = 90^\circ$ involves side-on collisions. The equations that relate the observed differential cross section (DCS) for a given preparation ($d\sigma_\alpha^\beta/d\omega$) is given by: [57]

$$\frac{d\sigma_\alpha^\beta}{d\omega} = \sum_{k=0}^{2j_{\text{HD}}} \sum_{q=-k}^k (2k+1) [S_q^{\{k\}}(\theta)]^* A_0^{(k)} C_{kq}(\beta, \alpha) \quad (3)$$

where $C_{kq}(\beta, \alpha)$ are the modified spherical harmonics and extrinsic moments $A_0^{(k)}$ that defined the preparation in the laboratory frame are derived in Ref 57. The integral cross section can be obtained by integrating $d\sigma_\alpha^\beta/d\omega$ over the scattering and the azimuthal angles, hence depending only on β .

Fig. 2 shows the cross sections for different experimentally achievable extrinsic preparations of the HD

rotational angular momentum for an unpolarized H_2 molecule. The results for $\Delta j = -2$ are relatively featureless, and are identical to those shown in Ref. 38. In the Wigner threshold regime, no control can be attained for the integral cross section [59]. With increasing collision energy, however, $\beta = 0^\circ$ always leads to larger cross sections (by up to a factor of 2). The effect of $\beta = 90^\circ$, and $\beta = \text{mag}$ (magic angle) preparations is milder, leading to only small changes in the cross sections with respect to the unpolarized case.

For $\Delta j = -1$ the situation is similar for energies below the resonance. However, at the resonance the collision mechanism changes rather abruptly, and the $\beta = 0^\circ$ preparation, which implies head-on collision, leads to a sudden decrease of the cross section, by close to a factor of 5, the most extreme effect that could be observed for any preparation of a sharp $j = 2$ state. Since the $\beta = 0^\circ$ preparation is the same as collisions with $\Omega = 0$ exclusively, the fact that the S-matrix element that causes the resonance does not contain $\Omega = 0$ leads to the disappearance of the resonance.

Well above the resonance, at $E_{\text{coll}} \geq 0.6$ K, the effect somewhat reverts back to the behavior observed below the resonance, with $\beta = 0^\circ$ again leading to a slight increase in the cross section. To sum up, the alignment of \mathbf{j}_{HD} perpendicular to \mathbf{k} slightly enhance the cross section except at the resonance, where it brings about the suppression of the resonance as if it were switched off. The effect of other preparations $\beta = 90^\circ$ and $\beta = \text{mag}$ is relatively minor and, apparently, does not affect the resonance significantly, as far as the integral cross section is concerned.

Up to this point, we have shown that at the resonance there is a change in the collision mechanism, which can be used to control the cross section by changing the preparation of the HD rotational angular momentum. It has been demonstrated recently by Perreault *et al.* that it is possible to determine the DCS for different reagent preparations [35, 36], so we now shift our attention to investigating how the DCS is affected by state-preparation of the HD molecule. Fig. 3 shows the DCS as a function of the scattering angle and collision energy for $\Delta j = -1$. The isotropic DCS (with unpolarized collision partners) is shown in panel (a), which features a slight preference for forward scattering. In particular, the resonance appears as a sharp “ridge” with a clear preference for forward scattering. For $\beta = 0^\circ$, panel (b), the situation is completely different. First, the resonance completely vanishes, and at 0.1 K there are no marked changes or discontinuities in the energy dependence of the DCS. In addition, the shape of the DCS displays prominent forward and backward peaks irrespective of the collision energy. At low collision energies there is a third peak in the DCS that only survives for energies below 0.03 K. There is also a resonance at higher collision energies, around $E_{\text{coll}} \sim 5$ K, which unlike the 0.1 K resonance is slightly

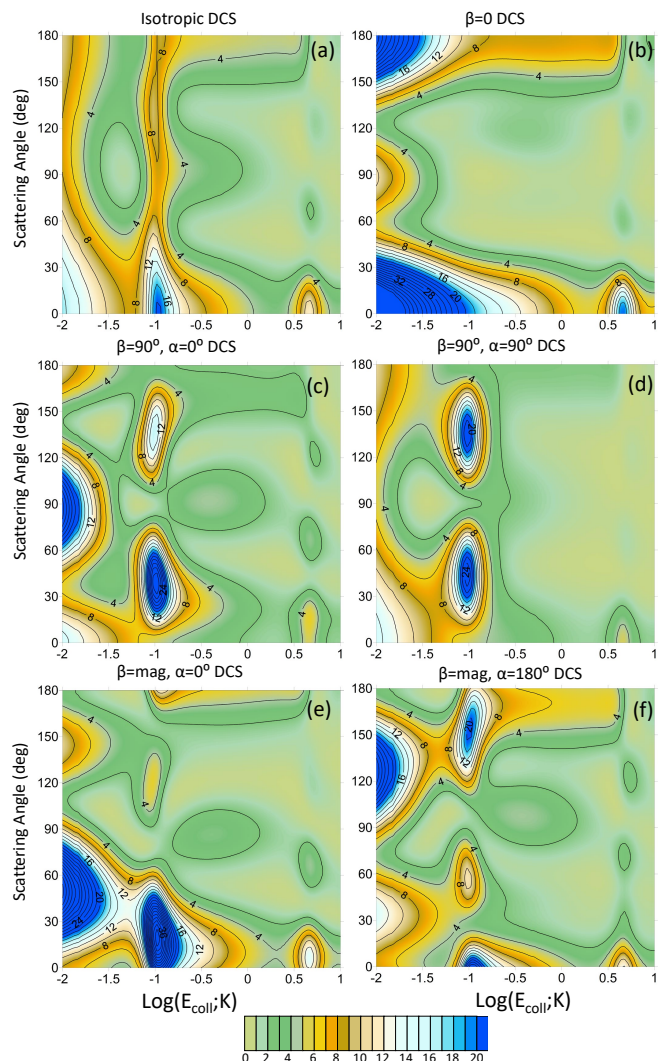


FIG. 3. Contour plots showing the collision energy dependence of the DCS for the $\Delta j = -1$ transition with different preparation of the HD rotational angular momentum. The angles β and α are the polar and azimuthal angles, respectively, that define the direction of the light polarization vector with respect to the \mathbf{k} - \mathbf{k}' scattering frame (where \mathbf{k} defines the z axis, and the reference plane contains \mathbf{k} and \mathbf{k}' , where \mathbf{k}' is the recoil velocity). While the integral cross sections at a given energy depends only on β , the DCS depends on both angles. The effect of the resonance is prominent for all preparations except for $\beta=0$, for which the resonance disappears.

enhanced by this external preparation.

While the $\beta = 90^\circ$ and $\beta = \text{mag}$ preparations have a minor effect on the integral cross section, the polarization of \mathbf{j}_{HD} has a dramatic effect on the shape of the DCS. Fig. 3 (panels (c)–(f)) shows the effect of $\beta = 90^\circ$ and $\beta = \text{mag}$ and $\alpha = 0^\circ, 180^\circ$ preparations on the DCS. The shape and magnitude of the DCS for all these cases differ from each other and from the isotropic case. Moreover, all of them show distinct features at the resonance. For $\beta = 90^\circ, \alpha = 0, 90^\circ$, the DCS at the resonance has

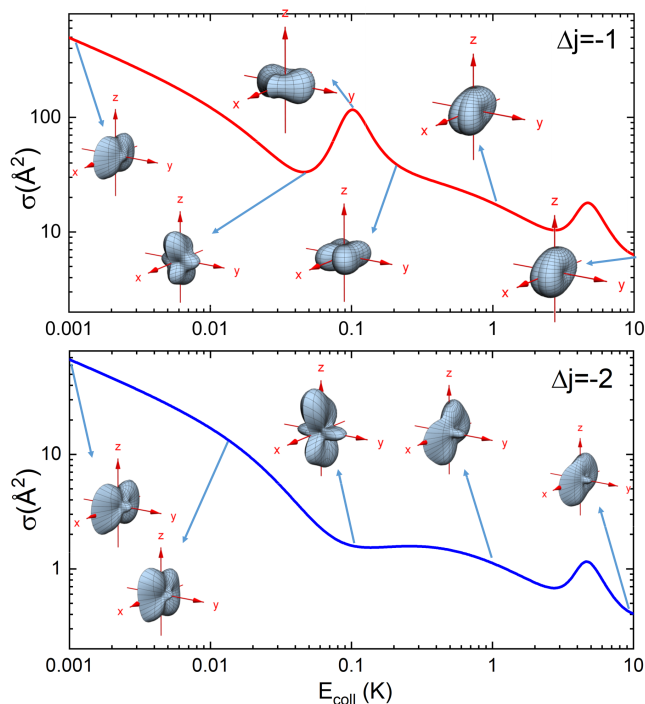


FIG. 4. Cross sections as a function of the collision energy for $\Delta j = -1$ (top panel) and -2 (bottom panel) along with the internuclear axis stereodynamical portraits (see text for further details) that reveal the change of mechanism at the resonance. The reference frame for the stereodynamical portraits is defined by the reactants approach (\mathbf{k}) and the products recoil (\mathbf{k}') directions. The z axis is parallel to \mathbf{k} , the x - z plane is the scattering plane, and y axis is parallel to $\mathbf{k} \times \mathbf{k}'$.

two prominent peaks at around 30° and 150° , while for $\beta = \text{mag}$ and $\alpha = 0^\circ$ there is a strong enhancement of forward scattering at the resonance. While for all non-zero β values the resonance at 0.1 K is present, its angular distribution is strongly sensitive to β , showing that the resonance can be used to control not just the magnitude of the cross section, but also the scattering direction. [32] This provides a powerful tool to elucidate stereodynamics of resonance-mediated collisions and fine-tune calculated interaction potentials against controlled experiments.

To gain further insight into the reaction mechanism we analyze the remaining polarization parameters besides $s_0^{(2)}$. For initial $j = 2$ there are 12 independent parameters of which 8 contribute to the alignment of the internuclear axis distribution. To aid the interpretation of these parameters we use “stereodynamical portraits” [60, 61], which show the spatial distribution of the angular momentum on the internuclear axis for a given polarization of the rotational angular momentum, with the z axis parallel to \mathbf{k} . Top panel of figure 4 presents the stereodynamical portraits associated with the internuclear axis of HD for $\Delta j = -1$. At the lowest energies considered here, the HD internuclear axis is contained in the scatter-

ing plane, although it does not show a significant preference towards head-on or side-on encounters. Just below the resonance, however, it starts to show a strong preference towards head-on collisions (typically associated with small impact parameters). A sudden change of the mechanism occurs at the resonance, with a clear preference for side-on encounters (internuclear axis perpendicular to z). Just above the resonance the internuclear axis remains perpendicular to the approach direction, but preferentially contained in the xy plane. With increasing collision energy, the internuclear axis is no longer aligned along or perpendicular to z . For $\Delta j = -2$, the stereodynamical portraits are similar except at the resonance found for $\Delta j = -1$ where, in contrast, the head-on encounters are preferred, evincing the dramatic change of the reaction mechanism caused by the resonance.

Altogether, these results demonstrate that, in the cold-energy regime, inelastic collisions between HD($v=1, j=2$) and p-H₂ are controlled by a resonance at 0.1 K that causes profound changes to the reaction mechanism that favors side-on collisions, typically associated with large impact parameters, over head-on collisions that would have been preferred if the resonance were absent. This sudden change in mechanism permits exquisite control of the collision outcome by using different preparations of the HD internuclear axis, and makes it possible to switch-off the resonance altogether. The effect of the initial HD alignment becomes most evident in the DCS, which changes dramatically for the alternative preparations investigated. Energy resolved measurements of angular distribution of state-prepared HD in collisions with H₂($v = 0, j = 0$) would be desirable to validate these predictions.

P.G.J. acknowledges funding by the Fundación Salamanca city of culture and knowledge (programme for attracting scientific talent to Salamanca). J.F.E.C. gratefully acknowledges support from the Dodd-Walls Centre for Photonic and Quantum Technologies. H. G. acknowledges US Department of energy (DE-SC0015997). M.B. thanks support of the UK EPSRC (to M.B. via Programme Grant EP/L005913/1). N.B. acknowledges support from the US National Science Foundation, Grant No. PHY-1806334. P.G.J. and F.J.A. acknowledges funding from the Spanish Ministry of Science and Innovation (Grants No. CTQ2015-65033-P and PGC2018-09644-B-100).

* pjambrina@usal.es

† j.croft@otago.ac.nz

‡ hguo@unm.edu

§ mark.brouard@chem.ox.ac.uk

¶ naduvala@unlv.nevada.edu

** aoiz@quim.ucm.es

[1] R. Wynar, R. S. Freeland, D. J. Han, C. Ryu, and D. J.

- Heinzen, *Science* **287**, 1016 (2000).
- [2] C. A. Regal, C. Ticknor, J. L. Bohn, and D. S. Jin, *Nature* **424**, 47 (2003).
- [3] B. C. Sawyer, B. L. Lev, E. R. Hudson, B. K. Stuhl, M. Lara, J. L. Bohn, and J. Ye, *Phys. Rev. Lett.* **98**, 253002 (2007).
- [4] E. S. Shuman, J. F. Barry, and D. DeMille, *Nature* **467**, 820 (2010).
- [5] M. T. Hummon, M. Yeo, B. K. Stuhl, A. L. Collopy, Y. Xia, and J. Ye, *Phys. Rev. Lett.* **110**, 143001 (2013).
- [6] N. Akerman, M. Karpov, Y. Segev, N. Bibelnik, J. Narevicius, and E. Narevicius, *Phys. Rev. Lett.* **119**, 073204 (2017).
- [7] L. Anderegg, B. L. Augenbraun, E. Chae, B. Hemmerling, N. R. Hutzler, A. Ravi, A. Collopy, J. Ye, W. Ketterle, and J. M. Doyle, *Phys. Rev. Lett.* **119**, 103201 (2017).
- [8] S. Truppe, H. Williams, M. Hambach, L. Caldwell, N. Fitch, E. Hinds, B. Sauer, and M. Tarbutt, *Nat. Phys.* **13**, 1173 (2017).
- [9] A. B. Henson, S. Gersten, Y. Shagam, J. Narevicius, and E. Narevicius, *Science* **338**, 234 (2012).
- [10] J. Jankunas, B. Bertsche, K. Jachymski, M. Hapka, and A. Osterwalder, *J. Chem. Phys.* **140**, 244302 (2014).
- [11] A. Klein, Y. Shagam, W. Skomorowski, P. S. Żuchowski, M. Pawlak, L. M. Janssen, N. Moiseyev, S. Y. van de Meerakker, A. van der Avoird, C. P. Koch, *et al.*, *Nat. Phys.* **13**, 35 (2017).
- [12] W. E. Perreault, N. Mukherjee, and R. N. Zare, *Chem. Phys.* **514**, 150 (2018).
- [13] C. Amarasinghe and A. G. Suits, *J. Phys. Chem. Lett.* **8**, 5153 (2017).
- [14] C. Naulin and M. Costes, *Int. Rev. Phys. Chem.* **33**, 427 (2014).
- [15] D. DeMille, J. M. Doyle, and A. O. Sushkov, *Science* **357**, 990 (2017).
- [16] J. J. Hudson, D. M. Kara, I. Smallman, B. E. Sauer, M. R. Tarbutt, and E. A. Hinds, *Nature* **473**, 493 (2011).
- [17] J. Baron, W. C. Campbell, D. DeMille, J. M. Doyle, G. Gabrielse, Y. V. Gurevich, P. W. Hess, N. R. Hutzler, E. Kirilov, I. Kozyryev, B. R. O’Leary, C. D. Panda, M. F. Parsons, E. S. Petrik, B. Spaun, A. C. Vutha, and A. D. West, *Science* **343**, 269 (2014).
- [18] W. B. Cairncross, D. N. Gresh, M. Grau, K. C. Cossel, T. S. Roussy, Y. Ni, Y. Zhou, J. Ye, and E. A. Cornell, *Phys. Rev. Lett.* **119**, 153001 (2017).
- [19] M. T. Bell and T. P. Softley, *Mol. Phys.* **107**, 99 (2009).
- [20] L. D. Carr, D. DeMille, R. V. Krems, and J. Ye, *New J. Phys.* **11**, 055049 (2009).
- [21] N. Balakrishnan, *J. Chem. Phys.* **145**, 150901 (2016).
- [22] J. L. Bohn, A. M. Rey, and J. Ye, *Science* **357**, 1002 (2017).
- [23] S. Ospelkaus, K.-K. Ni, D. Wang, M. H. G. de Miranda, B. Neyenhuis, G. Quémener, P. S. Julienne, J. L. Bohn, D. S. Jin, and J. Ye, *Science* **327**, 853 (2010).
- [24] N. Balakrishnan and A. Dalgarno, *Chem. Phys. Lett.* **341**, 652 (2001).
- [25] B. K. Kendrick, J. Hazra, and N. Balakrishnan, *Phys. Rev. Lett.* **115**, 153201 (2015).
- [26] R. B. Bernstein, D. R. Herschbach, and R. D. Levine, *J. Phys. Chem.* **91**, 5365 (1987).
- [27] R. D. Levine and R. B. Bernstein, *Molecular Reaction Dynamics and Chemical Reactivity* (Oxford University Press, 1987).
- [28] A. J. Orr-Ewing and R. N. Zare, *Annu. Rev. Phys. Chem.* **45**, 315 (1994).
- [29] A. J. Orr-Ewing, *J. Chem. Soc. Faraday Trans.* **92**, 881 (1996).
- [30] F. J. Aoiz, M. Brouard, S. D. S. Gordon, B. Nichols, S. Stolte, and V. Walpole, *Phys. Chem. Chem. Phys.* **17**, 30210 (2015).
- [31] T. R. Sharples, J. G. Leng, T. F. M. Luxford, K. G. McKendrick, P. G. Jambrina, F. J. Aoiz, D. W. Chandler, and M. L. Costen, *Nat. Chem.* **10**, 1148 (2018).
- [32] C. G. Heid, V. Walpole, M. Brouard, P. G. Jambrina, and F. J. Aoiz, *Nat. Chem.*, doi:10.1038/s41557.
- [33] F. Wang, K. Liu, and P. Rakitzis, *Nat. Chem.* **4**, 636 (2012).
- [34] F. Wang, J.-S. Lin, and K. Liu, *J. Chem. Phys.* **140**, 084202 (2014).
- [35] W. E. Perreault, N. Mukherjee, and R. N. Zare, *Science* **358**, 356 (2017).
- [36] W. E. Perreault, N. Mukherjee, and R. N. Zare, *Nat. Chem.* **10**, 561 (2018).
- [37] J. F. E. Croft, N. Balakrishnan, M. Huang, and H. Guo, *Phys. Rev. Lett.* **121**, 113401 (2018).
- [38] J. F. E. Croft and N. Balakrishnan, *J. Chem. Phys.* **150**, 164302 (2019).
- [39] M. P. de Miranda and D. C. Clary, *J. Chem. Phys.* **106**, 4509 (1997).
- [40] S. A. Kandel, A. J. Alexander, Z. H. Kim, R. N. Zare, F. J. Aoiz, L. Bañares, J. F. Castillo, and V. S. Rbanos, *J. Chem. Phys.* **112**, 670 (2000).
- [41] P. G. Jambrina, J. Aldegunde, F. J. Aoiz, M. Sneha, and R. N. Zare, *Chem. Sci.* **7**, 642 (2016).
- [42] J. Aldegunde, F. Javier Aoiz, and M. P. de Miranda, *Phys. Chem. Chem. Phys.* **10**, 1139 (2008).
- [43] P. G. Jambrina, M. Menéndez, A. Zanchet, E. Garcia, and F. J. Aoiz, *Phys. Chem. Chem. Phys.*, doi:10.1039/C8CP06892E (2019).
- [44] M. Brouard, H. Chadwick, C. J. Eyles, B. Hornung, B. Nichols, F. J. Aoiz, P. G. Jambrina, and S. Stolte, *J. Chem. Phys.* **138**, 104310 (2014).
- [45] A. M. Arthurs and A. Dalgarno, *Proc. Roy. Soc., Ser. A* **256**, 540 (1960).
- [46] J. Schaefer and W. Meyer, *J. Chem. Phys.* **70**, 344 (1979).
- [47] S. K. Pogrebnya and D. C. Clary, *Chem. Phys. Lett.* **363**, 523 (2002).
- [48] G. Quémener, N. Balakrishnan, and R. V. Krems, *Phys. Rev. A* **77**, 030704 (2008).
- [49] J. Schaefer, *Astronomy and Astrophysics Supplement Series* **85**, 1101 (1990).
- [50] D. R. Flower, *J. Phys. B – At. Mol. Opt. Phys.* **32**, 1755 (1999).
- [51] N. Balakrishnan, J. F. E. Croft, B. H. Yang, R. C. Forrey, and P. C. Stancil, *Astrophys. J* **866**, 95 (2018).
- [52] R. Krems, TwoBC – quantum scattering program, University of British Columbia, Vancouver, Canada, 2006.
- [53] G. Quémener and N. Balakrishnan, *J. Chem. Phys.* **130**, 114303 (2009).
- [54] R. J. Hinde, *J. Chem. Phys.* **128**, 154308 (2008).
- [55] M. H. Alexander and A. E. DePristo, *J. Chem. Phys.* **66**, 2166 (1977).
- [56] J. Aldegunde, M. P. de Miranda, J. M. Haigh, B. K. Kendrick, V. Saez-Rabanos, and F. J. Aoiz, *J. Phys. Chem. A* **109**, 6200 (2005).

- [57] J. Aldegunde, M. P. de Miranda, J. M. Haigh, B. K. Kendrick, V. Sáez-Rábanos, and F. J. Aoiz, *J. Phys. Chem. A* **109**, 6200 (2005).
- [58] J. Aldegunde, D. Herraes-Aguilar, P. G. Jambrina, F. J. Aoiz, J. Jankunas, and R. N. Zare, *J. Phys. Chem. Lett.* **3**, 2959 (2012).
- [59] J. Aldegunde, J. M. Alvarino, M. P. de Miranda, V. Saez Rabanos, and F. J. Aoiz, *J. Chem. Phys.* **125**, 133104 (2006).
- [60] M. P. de Miranda and F. J. Aoiz, *Phys. Rev. Lett.* **93**, 083201 (2004).
- [61] M. P. de Miranda, F. J. Aoiz, V. Sáez-Rábanos, and M. Brouard, *J. Chem. Phys.* **121**, 9830 (2004).